

Research of thermal stability of a-C:H and ta-C coatings

Zhihong Huang ^a, Wenchang Lang

Wenzhou Vocational & Technical College, Wenzhou 325035, China.

^a13600045268@126.com

Abstract

To assess the feasibility of a-C:H and ta-C coatings as protection coating for cutting tools, the a-C:H and ta-C coatings were deposited on the M2 high-speed steel substrate using the radio frequency PECVD and FCVA methods, respectively. The two DLC coatings were annealed in the atmosphere. The structure and mechanical properties of the coating were characterized by scanning electron microscope, atomic force microscope, Raman spectrum and nanometer indentation. Results: At 500 °C, the surface of the a-C:H coating got coarse and the ta-C coating was peeled off. Raman analysis showed that after annealing at 300 and 400 °C, the G peak position of the a-C:H coating increased from 1553 to 1565 and 1568 cm⁻¹, and ID/IG increased from 1.0 to 1.3 and 1.5; The G peak position of the ta-C coating increased from 1545 to 1557 and 1560 cm⁻¹, ID/IG increased from 0.7 to 0.9 and 1.1. The hardness of the as-deposited a-C:H and ta-C coating samples was 24.8 and 28.7 GPa, respectively. After 400 annealing, the hardness of the a-C:H coating decreased to 20.0 GPa, while the ta-C coating remained at 30.8 GPa. Conclusion: The application temperature of a-C:H coating and ta-C does not exceed 500 °C in atmospheric environment. As the temperature increasing, the a-C:H and ta-C coatings are gradually graphitized, but the ta-C coating is less graphitized than the a-C:H coating. The temperature increase significantly reduced the a-C:H coating, but the hardness of the ta-C coating did not change much. The ta-C coating was a more promising cutting tool protection coating.

Keywords

DLC, a-C:H, ta-C, Friction, Wear, Graphitization, Annealing.

1. Introduction

Diamond-like carbon(DLC) is a kind of amorphous carbon film material with low friction coefficient, high hardness, high chemical stability and high wear resistance[1]. The tribological properties of DLC coatings have led to the successful application of DLC coatings in the automotive industry to reduce energy losses and increase the life of key components[2]. DLC coatings have been widely used mainly include hydrogenated amorphous carbon(a-C:H) and tetrahedral amorphous carbon(ta-C); Since the hydrogen content and microstructure are different, the a-C:H and ta-C coatings exhibit different friction and wear characteristics: the a-C:H coatings provide ultra-low friction in an inert or vacuum environment. The ta-C coating provides ultra-low friction and wear in the presence of oxygen, hydrogen, or water molecules[3, 4].

Compared with the wide application of DLC coating in the automotive industry, DLC has little application in the field of surface protection of metal cutting tools. Because the DLC coating has good adhesion resistance under no lubrication conditions, the DLCcoating was once considered to be an ideal coating for aluminum alloy dry processing. At present, a lot of work has been done on the application and research of DLC in tools. However, some researchers report that DLC improves cutting performance[5-7], while other researchers found no effect[8]. This is due to large differences in the composition, structure, and mechanical properties of DLC coatings due to different deposition methods, process parameters, and the use of various precursors[9, 10]. Therefore, it is very difficult to choose what kind of DLC is used as a cutting tool coating.

It should be noted that the coating is affected by high temperature and environmental atmosphere during metal cutting. Therefore, it is necessary to understand the stability of DLC coating in high temperature and atmospheric environment. In this work, we prepared a-C:H and ta-C coatings, annealed at different temperatures in the atmosphere, characterized the structure and properties of the coatings, and explored the feasibility of applying DLC coatings to surface protection of cutting tools.

2. Experiment

2.1 Sample preparation

The sample is M2 high-speed steel, polished to the mirror with 1 μm diamond sandpaper, cleaned with alcohol and acetone ultrasound bath before coating, and dried with nitrogen. The a-C:H coating was deposited by plasma-enhanced chemical vapor deposition (PECVD) process. The ta-C coating was deposited by bending tube magnetic filtration cathode vacuum arc evaporation (FCVA) process.

A-C:H coating was deposited with MDC 600 vacuum coating system. The system is equipped with capacitive coupled radio frequency (RF, 13.56 MHz) plasma power supply. The substrate is a cathode, and tetramethylsilane (TMS) and acetylene (C_2H_2) are precursor gases. Before deposition, the sample was etched in an argon hydrogen plasma environment for 30 minutes. In order to further increase adhesion, TMS was introduced into the discharge chamber and an interlayer of $\text{Si}_x\text{C}_y\text{H}_z$ was deposited on the surface of the substrate. And then, gradually introducing the C_2H_2 , reducing the TMS flow and adjusting the bias output to deposit a layer of $\text{Si}_x\text{C}_y\text{H}_z$ coating with Si content gradient changes. When the TMS flow is reduced to 0 and the C_2H_2 reaches the default value, the deposition parameter is maintained and a top-layer a-C:H coating was deposited. The deposition parameters of the films are shown in Table 1.

Table 1 Process parameters for the deposition of the a-C:H coating

Process parameters	Pressure (mPa)	TMS flow rate (sccm)	C_2H_2 flow rate (sccm)	Bias Voltage (V)	Time (s)
$\text{Si}_x\text{C}_y\text{H}_z$ layer	100	200-0	0-600	-400	600
a-C:H layer	150	0	600	-600	3600

The ta-C coating was deposited by a NTC300 vacuum coating system. The equipment is equipped with an anode layer ion source, a magnetron sputtering titanium cathode and a bending tube magnetic filtration graphite arc cathode. Before deposition, the substrate is first etched with an anode ion source for 30 minutes, then the titanium adhesive layer is sputtering with a titanium target, and finally the ta-C coating is deposited with a graphite target. The C ions produced by the graphite arc target are focused by the coil around the outer wall of the bend, transported along the bend to a deflection coil between the bend and the vacuum chamber. The deflection coil is passed through the alternating current, and an ion beam scan is produced. The scanning range is 120mm, frequency is 1Hz; The workpiece is installed on a rotating holder in a vacuum chamber at a speed of 3 rpm. The deposition parameters of the films are shown in Table 2.

Table 2 Process parameters for the deposition of the ta-C coating

Process parameters	Pressure (mPa)	Ar flow rate (sccm)	Ti target current (A)	C target current (A)	Bias Voltage (V)	Time (s)
Ti layer	30	Pressure control	20	0	-100	600
ta-C layer	-	0	0	60	0	3600

The as-deposited sample was annealed in a Muffle furnace in an atmospheric environment. The annealing temperature is 300, 400, 500, 600 and 700 $^\circ\text{C}$. The warming speed is 50 $^\circ\text{C}\cdot\text{min}^{-1}$, the insulation time is 1 hour.

2.2 Characterization

- 1) Field emission scanning electron microscopy (FESEM, Zeiss SigmaHD) was used to characterize the cross-section morphology and measure the thickness of the coating.
- 2) The surface morphology of the coating was characterized by a CSPM4000 atomic force microscope (AFM) with a scanning area of $25\ \mu\text{m} \times 25\ \mu\text{m}$ and a scanning frequency of 5 Hz.
- 3) The Raman spectrum was measured using Renisaw RM-1000 laser confocal Raman spectrometer with an Ar-ion laser of a wavelength of 514.5 nm and a scanning range of 500 to 2000 cm^{-1} .
- 4) The hardness and elastic modulus of the coating were determined by MTS-NanoG200 nanometer indenter under continuous stiffness mode.

3. Result and discussion

3.1 The morphology and antioxidant properties of a-C:H and ta-C coatings

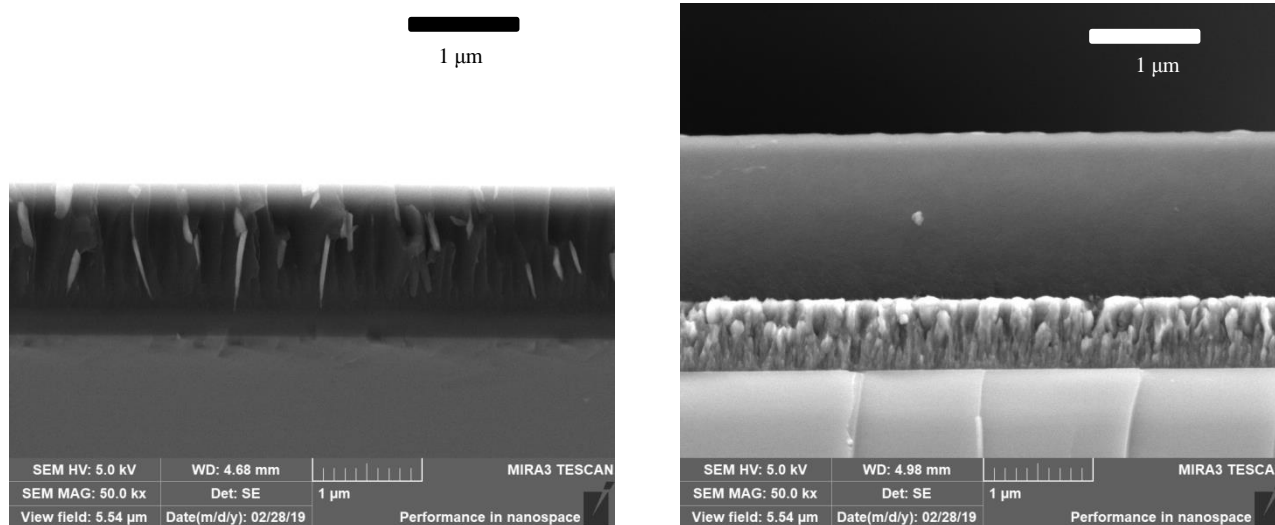


Fig.1. Cross-section SEM images of the a-C:H and ta-C coatings

Fig. 1 is a cross-section SEM photograph of a-C:H and ta-C coatings. The thickness of the a-C:H coating is $1.4\ \mu\text{m}$, including a gradient interlayer of $0.2\ \mu\text{m}$ and a carbon layer of $1.2\ \mu\text{m}$. The interlayer and the carbon layer are both amorphous structures. The transition of the interlayer carbon layer is very coherent. There are some cracks in the carbon layer vertical to the interface. The cracks disappear in the interface between the interlayer and the function layer without penetrating the interlayer. The ta-C coating has a thickness of $2.2\ \mu\text{m}$, including a metal Ti interlayer of $0.7\ \mu\text{m}$ and a carbon layer of $1.5\ \mu\text{m}$. The Ti interlayer is a columnar crystal structure, the carbon layer is amorphous, and there is no crack in the cross section.

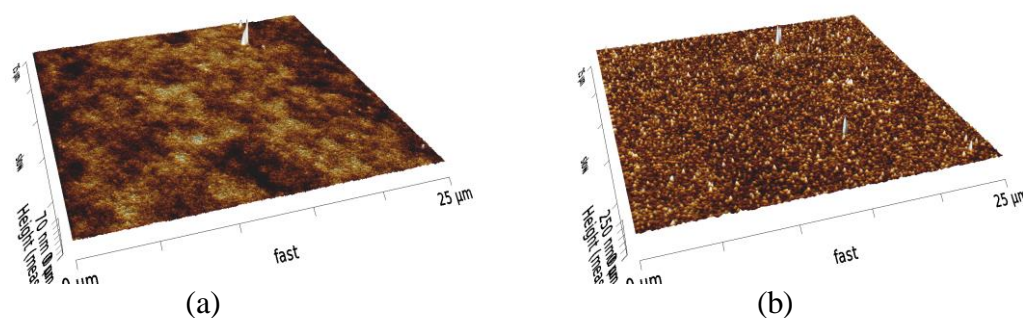


Fig.2 AFM image of a-C:H and ta-C coatings

Fig. 2 are the surface AFM images of a-C:H and ta-C coatings. The surface roughness of the a-C:H coating is RMS 27.2 nm, the average cluster diameter is 92 nm, the surface roughness of the ta-C coating is RMS 28.2 nm, and the average cluster diameter is 184 nm. Although the ta-C coating is deposited with a carbon ion beam filtered by a magnetic field, average cluster diameter of the ta-C coating is still much higher than that of the a-C:H coating deposited by the CVD method.

The a-C:H and ta-C samples were annealed in a Muffle furnace in the atmospheric environment, the surface of the a-C:H and ta-C coating samples annealed at 300 and 400 °C was not significantly different from the as-deposited samples. The surface of the a-C:H coating samples annealed at 500, 600 and 700 °C showed obvious coarseness. The ta-C sample annealed at 500 °C was peeled off suddenly during treatment, and the ta-C sample surface annealed at 600 and 700 °C had no coatings. When annealed at 500 °C, the surface roughening of the a-C:H coating and the peel-off of the ta-C coating showed that the temperature resistance of the a-C:H and ta-C coatings did not exceed 500 °C.

3.2 Raman spectra of a-C:H and ta-C coatings

The graphitization of DLC coatings during annealing will weaken the shear strength of the coatings. Raman spectroscopy is a very powerful tool for studying the graphitization process of carbon films. The Raman spectrum of the DLC coating consists of the G peak(1580 cm^{-1}) and the D peak(1350 cm^{-1}). The G peak corresponds to the SP² carbon bond, while the D peak is associated with the disorder of the graphite lattice(such as the grain boundary). In order to study the graphitization process, we carried out Raman analysis of a-C:H and ta-C coating samples.

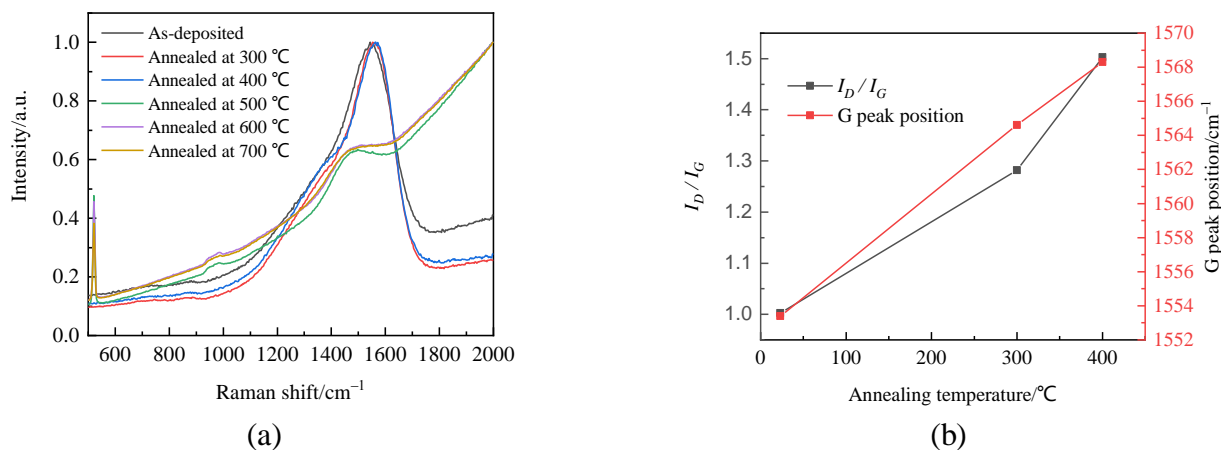


Fig. 3 Raman spectroscopy of a-C:H coatings

Fig. 3(a) is a normalized Raman map of the a-C:H coating. From the figure, it can be seen that the samples annealed at 500, 600 and 700 °C have a strong PL(photoluminescence) background. According to the study result of Casiraghi, etc.[11], the hydrogen content of the coating is proportional with the slope of the PL background, meaning that samples with annealing above 500 °C have a high hydrogen content. The C-H bond is stronger than the C-C bond, and the thermal desorption of hydrogen to carbon occurs above 700 °C[12, 13] With the increase of the annealing temperature, the C-C bond breaks before the C-H bond, and C combines with O in the atmosphere to form a CO₂ gas that volatiles from the coating, resulting in an increase in the hydrogen content of the coating. The loss of C resulted in the conversion of the a-C:H coating from DLC(diamond-like carbon) to PLC(polymer-like carbon)[14, 15], shows a strong PL back base in the Raman spectrum. Comparing the Raman spectra of the as-deposited, 300 and 400 °C annealed a-C:H coating samples, it can be found that the G peak position of the as-deposited sample is lower than 300 and 400 °C annealed samples. The G peak position of the 300 and 400 °C annealed samples is similar. However, there is a clear step in the D peak area in Raman spectra, indicating that after annealing the D peak and the G peak tend to separate, it can also be seen that the D peak component of the 400 °C annealed sample is higher than the 300 °C annealed sample. In order to understand more clearly the law of changes in the spectra, we used the Gaussian curve to fit the Raman spectra of the as-deposited and

the 300, 400 °C annealed samples after deducting the background, and the results were shown in Fig. 3(b). The G peak position of the as-deposited a-C:H coating sample is 1553 cm⁻¹ and ID/IG is 1.0; After 300 and 400 °C annealing, the G peak is increased to 1565 and 1568 cm⁻¹, and the ID/IG is increased to 1.3 and 1.5. The ID/IG and the G peak position increase indicate that the a-C:H coating is gradually graphitized as the annealing temperature increases.

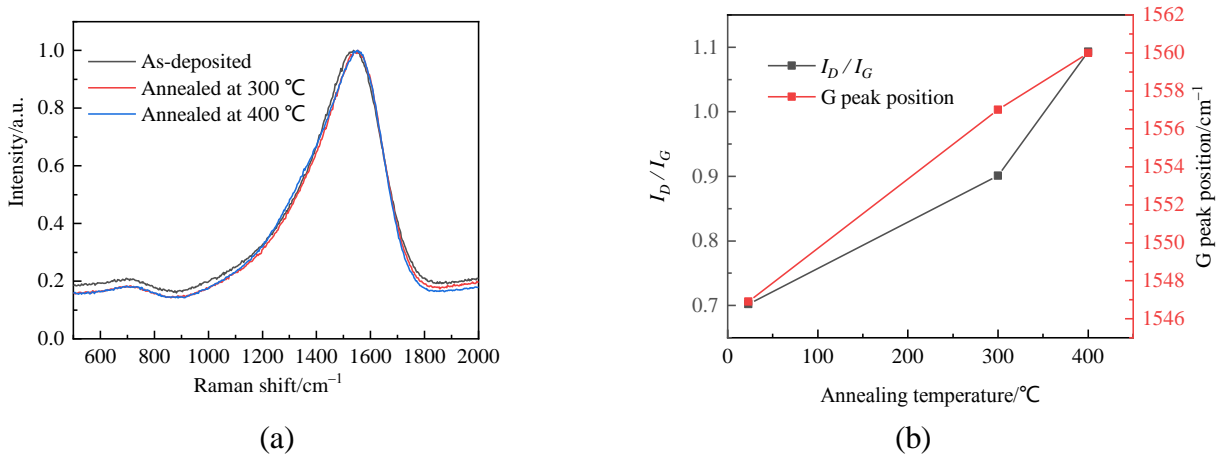


Fig. 4 Raman spectroscopy of ta-C coatings

The Raman spectra of the as-deposited ta-C coating sample and the annealed sample (Fig. 4a) are close to coincide, indicating that annealing results in a lower degree of graphitization of the ta-C coating. However, careful observation still shows that the G peak position of the as-deposited sample of the ta-C coating is lower than that of the annealed samples, and the D-peak component of the annealed sample at 400 °C is higher than the 300 degree annealed sample. The results of Gaussian curve fitting are shown in Fig. 4(b). After 300 and 400 °C annealing, the ID/IG of the ta-C coating increased from 0.7 to 0.9 and 1.1, and the G peak position increased from 1545 cm⁻¹ to 1557 and 1560 cm⁻¹. The ID/IG and the G peak position increase indicate that the ta-C coating is gradually graphitized as the annealing temperature increases, and the graphitization of the ta-C coating with temperature increases is less than that of the a-C:H coating.

3.3 Mechanical properties of a-C:H and ta-C coatings

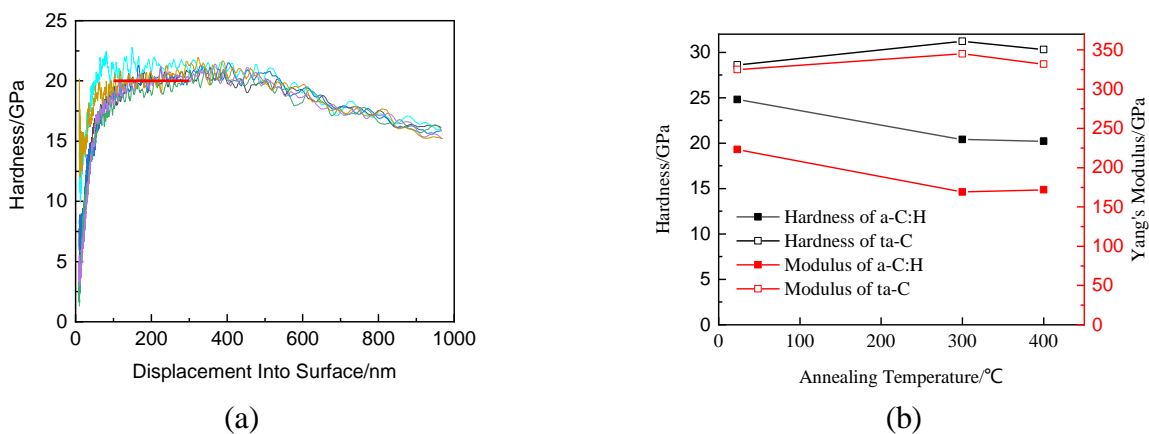


Fig. 5 Nanohardness of a-C:H and ta-C coatings

Hardness is the ability of the film to resist the pressure of foreign hard objects into its surface. Fig. 5(a) is the nanometer indentation hardness curve (300 °C annealing a-C:H coating) of the DLC coating in typical continuous stiffness mode. To avoid indentation size effect and basement effect occur, we select the average indentation hardness at a depth of about 200 nm as the hardness of the coating. The Nano hardness and elastic modulus of the coating are shown in Fig. 5(b).

The hardness of the as-deposited a-C:H and ta-C coating samples was 24.8 and 28.7 GPa, respectively. The ta-C has a higher hardness due to the fact that its composition does not contain hydrogen and has a higher SP³ C content. After annealing at 300 °C, the hardness of the a-C:H coating decreases by about 5GPa to 20.0 GPa, indicating that the graphitization of the a-C:H coating causes its hardness to decrease; When the annealing temperature rises to 400 °C, the hardness of the a-C:H coating no longer decreases. After annealing at 300 to 400 °C, the hardness of the ta-C coating remained basically unchanged or even slightly increased. Excluding sampling and measurement errors, it can be concluded that annealing significantly reduces the hardness of a-C:H, and has little effect on the hardness of the ta-C coating. This conclusion is consistent with the results of the Raman spectral analysis of annealing of a-C:H and ta-C coating samples, so that the ta-C coating has better thermal stability than the a-C:H coating.

4. Conclusion

The effective use temperature of a-C:H and ta-C coating in the atmosphere does not exceed 500 °C. At 500 °C, the a-C:H coating will transform structure from diamond-like to polymer-like, the ta-C coating will fail to adhere. Under 400 °C, the a-C:H coating and the ta-C coating will graphitize as the temperature increases, and the graphitization of the a-C:H coating is faster than that of ta-C. The hardness of the a-C:H coating decreased significantly with the increase of the temperature, while the hardness of the ta-C coating did not change much. The ta-C coating is a more potential dry cutting coating.

Acknowledgements

This work was supported by Wenzhou public welfare science and technology project under Grant No.G20160003.

References

- [1] J. Robertson: Diamond-like amorphous carbon[J]. *Materials science and engineering: R: reports*, 2002, 379(4-6): 129–281.
- [2] S. Lawes, S. Hainsworth, M. Fitzpatrick: Impact wear testing of diamond-like carbon films for engine valve-tappet surfaces[J]. *Wear*, 2010, 268(11–12): 1303–1308.
- [3] H. Ronkainen, S. Varjus, J. Koskinen, et al: Differentiating the tribological performance of hydrogenated and hydrogen-free DLC coatings[J]. *Wear*, 2001, 249(3-4): 260–266.
- [4] J. Andersson, R. A. Erck, A. Erdemir: Friction of diamond-like carbon films in different atmospheres[J]. *Wear*, 2003, 254(3-4): 1070–1075.
- [5] M. Lahres, P. Müller-Hummel, O. Doerfel: Applicability of different hard coatings in dry milling aluminium alloys[J]. *Surface and coatings technology*, 1997, 91(1-2): 116–121.
- [6] K. Enke: Dry machining and increase of endurance of machine parts with improved doped DLC coatings on steel, ceramics and aluminium[J]. *Surface and coatings technology*, 1999, 116–119: 488–491.
- [7] M. J. Dai, K. S. Zhou, Z. H. Yuan, et al: The cutting performance of diamond and DLC-coated cutting tools[J]. *Diamond and related materials*, 2000, 9(9-10): 1753–1757.
- [8] T. C. S. Vandeveld, K. Vandierendonck, M. V. Stappen, et al: Cutting applications of DLC, hard carbon and diamond films[J]. *Surface and coatings technology*, 1999, 113(1-2): 80–85.
- [9] A. Grill: Diamond-like carbon: state of the art[J]. *Diamond and related materials*, 1999, 8(2-5): 428–434.
- [10] A. C. Ferrari, J. Robertson: Interpretation of Raman spectra of disordered and amorphous carbon[J]. *Physical review*, 2000, B61(20): 14095–14107.
- [11] C. Casiraghi, A. C. Ferrari, J. Robertson: Raman spectroscopy of hydrogenated amorphous carbons[J]. *Physical review* 2005, B72(8): 85401-85414.
- [12] A. Erdemir: The role of hydrogen in tribological properties of diamond-like carbon films[J]. *Surface and coatings technology*, 2001, 146–147: 292-297.

- [13] C. Su, J. C. Lin: Thermal desorption of hydrogen from the diamond C(100) surface[J]. Surface science, 1998, 406(1-3): 149-166.
- [14] D. Y. Wang, C. L. Chang, W. Y. Ho: Oxidation behavior of diamond-like carbon films[J]. Surface and coatings technology, 1999, 120–121: 138-144.
- [15] M. C. Chiu, W. P. Hsieh, W. Y. Ho et al: Thermal stability of Cr-doped diamond-like carbon films synthesized by cathodic arc evaporation[J]. Thin Solid Films, 2005, 476(2) 258-263.